Important declarations

Please remove this info from manuscript text if it is also present there.

Associated Data

Data supplied by the author:
I am uploading both the raw and processed data used in this study.

Required Statements

Competing Interest statement:
The authors declare that they have no competing interests.

Funding statement:
Research reported in this publication was supported by (1) the Eunice Kennedy Shiver National Institute of Child Health & Human Development of the National Institutes of Health under Award Number K12HD073945, (2) NSF CAREER Award #1944001, (3) a seed grant from the University of Tennessee Office of Research and Engagement, and (4) the University of Tennessee Department of Mechanical, Aerospace and Biomedical Engineering start-up funds.

Rabbit hindlimb kinematics and ground contact pressure during the stance phase of hopping gait

Patrick Hall [Corresp., 1], **Caleb Stubbs** [1], **David E Anderson** [2], **Cheryl B Greenacre** [3], **Dustin L Crouch** [1]

[1] Mechanical, Aerospace, and Biomedical Engineering, University of Tennessee - Knoxville, Knoxville, Tennessee, United States

[2] Department of Large Animal Sciences, University of Tennessee - Knoxville, Knoxville, Tennessee, United States

[3] Department of Small Animal Sciences, University of Tennessee - Knoxville, Knoxville, Tennessee, United States

Corresponding Author: Patrick Hall
Email address: phall8@vols.utk.edu

Though the rabbit is a common animal model in musculoskeletal research, there is very limited data reported on healthy rabbit biomechanics. Our objective was to quantify the normative hindlimb biomechanics of six New Zealand White rabbits during the stance phase of hopping gait. We measured biomechanics by synchronously recording sagittal plane motion and ground contact pressure using a video camera and pressure mat, respectively. The range of motion of the foot angle and ankle angle during stance phase were 108.9 degrees and 78.1 degrees, respectively. The maximum vertical ground reaction force and contact area, both averaged across rabbits, were 42.5 +/- 11.4 %BW and 7.5 +/- 1.8cm^2, respectively. Rabbits are generally considered as having a plantigrade gait pattern, like humans; our study confirms this. However, unlike humans, rabbits never have a negative foot angle (i.e., "toes up") with respect to the ground during stance. Future studies can reference our data to quantify the extent to which orthopedic interventions affect rabbit biomechanics.

Rabbit Hindlimb Kinematics and Ground Contact Pressure During the Stance Phase of Hopping Gait

Authors: Patrick T. Hall[1], Caleb Stubbs[1], David E. Anderson[2], Cheryl B. Greenacre[3], Dustin L. Crouch[1]

[1]University of Tennessee, Knoxville – Department of Mechanical, Aerospace, and Biomedical Engineering

[2]University of Tennessee, Knoxville – Department of Large Animal Sciences

[3]University of Tennessee, Knoxville – Department of Small Animal Sciences

Corresponding author contact:

Phone: (615) 815-9431

Email: phall8@vols.utk.edu

Keywords: Rabbit, Biomechanics, Noninvasive, Stance

Word Count: 2827

Abstract

Though the rabbit is a common animal model in musculoskeletal research, there is very limited data reported on healthy rabbit biomechanics. Our objective was to quantify the normative hindlimb biomechanics of six New Zealand White rabbits during the stance phase of hopping gait. We measured biomechanics by synchronously recording sagittal plane motion and ground contact pressure using a video camera and pressure mat, respectively. The range of motion of the foot angle and ankle angle during stance phase was 108.9 degrees and 78.1 degrees, respectively. The maximum vertical ground reaction force and contact area, both averaged across rabbits, were 42.5 ± 11.4 %BW and 7.5 ± 1.8 cm^2, respectively. Rabbits are generally considered as having a plantigrade gait pattern, like humans; our study confirmed this. However, unlike humans, rabbits never have a negative foot angle (i.e., “toes up”) with respect to the ground during stance. Future studies can reference our data to quantify the extent to which orthopedic interventions affect rabbit biomechanics.

Introduction

The rabbit is a common animal model in musculoskeletal research to, for example, test new potential clinical interventions or study the response of tissues to mechanical stimuli. Some interventions would be expected to affect the motor function of the hindlimb ankle and foot. Examples of such interventions include tenotomy of ankle dorsiflexor muscles (Abrams et al. 2000) or the Achilles tendon (Nagasawa et al. 2008; Reddy et al. 1998), immobilization of the knee and/or ankle joint (Gossman et al. 1986; Ponten & Friden 2008; Sjostrom et al. 1979), and release of tendon retinacula to manipulate muscle-tendon moment arms (Koh & Herzog 1998b; Reddy & Gupta 2007). Recently, we adopted a rabbit model to test the feasibility of a new type of ankle-foot prosthesis (Hall et al. 2020b). For these interventions, it may be valuable and informative to quantify their effect on motor function.

One way to quantify motor function is by measuring biomechanical variables, such as kinematics and ground reaction forces. The effect of an intervention could be determined by comparing biomechanical data between animals that did and did not receive the intervention. Unfortunately, very little data has been reported on the hindlimb biomechanics of healthy rabbits. We are aware of only one previous study that reported rabbit biomechanics during hopping gait, and multi-sample data were limited to knee and ankle joint moments (Gushue et al. 2005). A more comprehensive dataset on normative rabbit hindlimb biomechanics in the literature would (1) make it easier for researchers to determine the effects of experimental interventions on motor function, (2) reduce the number of healthy animals used as experimental controls, and (3) increase basic understanding about animal locomotion.

Two commonly reported measures of hindlimb biomechanics that have not been reported for a multi-sample rabbit cohort are joint kinematics and ground contact pressure, which provide valuable information about limb motion and loading, respectively. Like for the lower extremity during walking gait in humans, rabbits are thought to exhibit a plantigrade

hopping gait style (Bensley 1910; T 1996) in which most or all of the plantar surface of the hindlimb foot contacts the ground during the stance phase. Thus, we expect that rabbits and humans would exhibit similar kinematics at the ankle and foot during stance. For example, during the stance phase of walking, the human ankle angle transitions nearly linearly from dorsiflexion to plantarflexion (Kadaba et al. 1990). One previous study reported the net vertical ground reaction force (i.e., integral of ground contact pressure across the contact area) for one rabbit (Gushue et al. 2005); the data suggest that rabbits, like humans (Wannop et al. 2012), exhibit a bimodal net ground reaction force pattern during stance. Ground contact pressure data would complement net ground reaction force data by revealing the spatiotemporal distribution of forces on the foot.

The goal of our study was to quantify ankle and foot kinematics and ground contact pressures during the stance phase of hopping gait in healthy rabbits (i.e., rabbits that have not received an experimental intervention). We expected that rabbits would exhibit plantigrade gait characteristics during stance, similar to humans. Summary results are presented below, and the raw data are attached in supplementary data. The new biomechanics data will serve as a valuable reference for experimental interventions and improve our understanding about rabbit locomotion.

Materials & Methods

Subjects

All procedures were approved by the University of Tennessee, Knoxville Institutional Animal Care and Use Committee. We used six 14-week-old New Zealand White (NZW) Rabbits (weight = 2.7 ± 0.33kgs). During the two-week acclimation period prior to testing, rabbits were trained to hop through an acrylic tunnel when given negative reinforcement (i.e., prodding). Rabbits were housed in pairs and given daily enrichment and positive human interaction.

Instrumentation and Setup

The setup for our locomotor measurement system included several components (Fig. 1, 1-3). A pressure mat (Tekscan, Very HR Walkway 4; South Boston, MA) was used to record pressure data at 60 Hz. We taped 320-grit sandpaper to the top of the smooth pressure-sensing area to prevent the rabbits from slipping. We placed a 3-kg weight on the sandpaper-covered mat and calibrated the mat through the Tekscan software calibration program. The mat was placed inside a clear acrylic tunnel to guide the rabbits across the pressure mat. The mat width (11.2 cm) permitted only unilateral pressure measurements; therefore, to record data for both hindlimbs, we laterally offset the mat in the tunnel and had the rabbit hop across the mat in both directions (see Testing Procedure below). A camera (1080P HD Webcam, SVPRO), placed three feet away from the clear acrylic panel, captured video at 60 Hz. Video and pressure mat data were synchronized using the Tekscan Walkway software (Tekscan, South Boston, MA).

Testing Procedure

Before testing, we shaved both hindlimbs and marked the metatarsophalangeal (MTP), ankle, and knee joint centers on the lateral side of each hindlimb with black ink (Fig. 1, 4). The marks were made so that we could identify the joint locations during the kinematics analysis described below. After marking, we placed the rabbit into a pen with the acrylic tunnel and pressure mat. Each trial began when the rabbit entered the tunnel. A trial was deemed successful if the rabbit continued the hopping motion through the entire length of the tunnel without stopping. The rabbits completed 5 trials of hopping through the tunnel in each direction while we synchronously recorded pressure and video data for each trial. The summary data for each rabbit included all 5 trials from both hindlimbs (10 trials total per rabbit).

Data Processing

We calculated joint angles from the video frames corresponding to stance phase using a custom motion analysis program written in MATLAB (Mathworks, Natick, MA). The program

used a bottom-hat morphology filter to distinguish the black ink marks and calculate the centroid of each marker position (Fig. 2). Then, frame-by-frame, we visually verified the marker centroids and, if the centroid location appeared inaccurate, corrected the location by manually approximating the centroid from the still frame. This method assumed that the sagittal plane orientation of the foot and shank was aligned with the line segments connecting the centroids; this was a reasonable assumption given the arrangement of the camera with respect to the acrylic tunnel. Finally, we calculated the angle between the foot segment and ground (i.e., foot angle) and between the foot and shank segments (i.e., ankle angle) throughout stance (Fig. 2). Since the camera was approximately level with the ground, we defined the ground as the horizontal line that intersected the MTP joint.

Evaluating joint angles separately for each joint provides an incomplete picture of rabbit hindlimb kinematics. This is because the hindlimb is a kinematic chain, so the positions and orientations of proximal limb segments depend on those of distal limb segments. Therefore, we calculated the knee joint center position in the sagittal plane from the foot and ankle angles. To permit comparison among rabbits of different sizes, we applied the joint angles to a geometrically normalized model of the rabbit hindlimb (Fig. 3, A). The foot and shank segments of the model were 2 and 3 normalized length units (NLUs), respectively, to approximate the anatomical length proportions between the two segments. With respect to the anthropometry of the rabbits in our study, 1 NLU represents approximately 3.3 cm. For each rabbit, we computed the time-series “trajectory” of knee joint position throughout stance for each trial.

Ground contact pressure data were processed using the Tekscan Walkway software. Each hind foot was isolated by drawing a strike box around the foot contact location, as indicated by the pressure data (Fig. 4). From the pressure data in the strike box and for each time point, we computed (1) average pressure, (2) contact area, and (3) net vertical ground reaction force (vGRF). The contact area was calculated as the total geometric area within the

strike box for which the pressure was greater than zero. The vGRF was calculated as the product of foot contact area and the average pressure across the contact area. We also computed the total contact area over the entire stance phase. The duration of the stance phase for each limb was computed as the length of time for which pressure was greater than zero within the limb's strike box.

Bilateral Comparison

Since our setup limited data collection to one side at a time, we compared data between sides to identify potential bias. In each trial, the timepoints were normalized by the duration of stance phase, permitting comparison among trials of different stance durations. We averaged time-series joint angles, vGRFs, contact areas, and contact pressures across all rabbits for each hindlimb (right and left) and normalized the vGRF by body weight (%BW). We compared the averaged time-series data between the right and left limbs using statistical parametric mapping (SPM), with $\alpha=0.05$ (Pataky 2010). We used a paired Student's t-test to compare stance duration between the right and left hindlimb.

To compare knee joint center trajectories bilaterally, we first averaged data across trials separately for the right and left hindlimb. Next, we calculated the Euclidean distance between the averaged right and left hindlimb trajectories at every one percent of stance. We used SPM ($\alpha=0.05$) to identify portions of stance for which the Euclidean difference was significantly different from zero, which would indicate a significant difference in knee joint position between hindlimbs.

Results

Joint Kinematics

The summary kinematics, averaged across all 6 rabbits and both sides, showed that the foot angle ranged from 15-123.9 degrees and the ankle angle ranged from 67.6-135.7 degrees

(Fig. 5). The ankle angle started with a negative slope and switched to a positive slope at approximately 40% of stance; this point of peak dorsiflexion (i.e., lowest) ankle angle divided the stance phase into loading response and forward propulsion sub-phases, as with human stance (Li & Hsiao-Wecksler 2013). The standard deviation of the foot and ankle angles, averaged over the stance phase, were 7.32 and 12.36 degrees, respectively. When comparing between right and left hindlimbs, SPM revealed no significant kinematic differences in either joint angle.

In general, during stance, the knee joint center gradually progressed approximately 1.5 NLUs downward and 5.5 NLUs forward. The standard deviation in normalized knee joint center position, averaged across rabbits, was approximately 1 NLU. The average Euclidean distance between right and left knee joint centers during stance ranged from 0.39 - 0.78 NLUs (Fig. 6). The distance was significantly different from zero throughout stance, with the largest differences occurring during the first 25% of stance phase. Though the *distance* between knee joint centers was significantly different from zero, the *trajectory* of the knee joint center in the sagittal plane was qualitatively similar between sides (Fig. 3, B).

Ground Contact Pressure

The summary ground reaction data showed that rabbits experienced a maximum vGRF of 42.5 ± 11.4 %BW and the contact area reached a maximum of 7.5 ± 1.8 cm^2 (Fig. 7). Both the vGRF and contact area showed similar bimodal trends during stance, with the first peak occurring at approximately 25% of stance and the second occurring at approximately 75% of stance. In fact, vGRF and contact area were strongly correlated, with a Pearson's correlation coefficient of 0.986. Because of the correlation between vGRF and contact area, the foot experienced a nearly constant average pressure of approximately 0.15 kg/cm^2 through the middle 80% of stance (Fig. 7).

When comparing the right and left hindlimbs, the vertical ground reaction force (vGRF) was 4.9-5.9 %BW larger ($p = 0.048$) for the right leg (36.4%±7.9 %BW) than the left leg

(31.4±8.5 %BW) for only a small portion (48-50%) of stance (Fig. 4). There was no significant bilateral difference in average pressure or contact area during stance (Fig. 5). Stance duration was not significantly different (p=0.38) between the right (0.46 ± 0.16 s) and the left (0.54 ± 0.16 s) hindlimbs.

Discussion

Rabbits have been considered as plantigrade(Bensley 1910; T 1996), while other common research animal models are either digitigrade (e.g. cats, dogs)(Barbeau & Rossignol 1987) or unguligrade (e.g. pigs and goats) (Polly 2007). Our kinematic and pressure data confirmed that rabbits exhibit a plantigrade gait pattern, loading the heel area first (Fig. 5). Humans also have a plantigrade walking pattern and land with their heel first (Grasso et al. 1998), though the foot angle is more negative during walking. Such differences must be considered when attempting to extrapolate results from animal studies to humans.

The time-series vGRF data exhibited a bimodal pattern that is consistent with vGRF data reported for one rabbit(Gushue et al. 2005) and for humans during walking(Wannop et al. 2012). We expect that, as with humans, the maximum vGRF that occurs at approximately 25% of stance corresponds to the loading response triggered by the need to support body weight during landing (Winiarski & Rutkowska-Kucharska 2009). As in humans (Grasso et al. 1998), the second mode at approximately 75% of stance presumably corresponds to forward propulsion, though we could not confirm this since the pressure mat cannot record horizontal ground reaction forces.

Contact area was strongly correlated with vGRF magnitude, with a correlation coefficient of 0.986 across all trials. The correlation explains why the average pressure was nearly constant throughout stance phase. Maintaining a constant ground-paw pressure may be a locomotor strategy employed by the rabbit's sensorimotor system. As seen in our prior study

(Hall et al. 2020a), orthopedic interventions can alter the pressure between the hindlimb and ground. When testing our endoprosthesis in the future, it will be interesting to see if rabbits adapt their hindlimb movement to preserve ground-foot pressure throughout stance phase.

We observed some bilateral biomechanical differences that were statistically significant: (1) a difference in vGRF over a very small (2%) portion of stance, and (2) the distance between right and left knee joint centers over most of stance. The differences may have been because we recorded data separately for each hindlimb, a limitation noted below. Alternatively, the observed bilateral differences may have been due to limb preference, though this is not possible to conclude from our dataset given our setup limitations and small sample size.

We computed the sagittal-plane position of the knee joint center, which gives an indication of how the joint is moving in the global coordinate system. In contrast, joint angles represent the orientation of one local coordinate frame to another, where both frames are aligned with a limb segment. Thus, joint center position data provide important context to joint angle data by showing how local joint-level changes may affect global limb or body position. Joint center positions may even better reflect task goals than joint angles. For example, a previous study found that rats with peripheral nerve injury recovered joint position kinematics even as individual joint angles remained altered (Chang et al. 2018).

Several techniques have been used to measure limb kinematics and ground reaction forces. The previous rabbit biomechanics study (Gushue et al. 2005) attached reflective motion capture markers to transdermal bone pins. This invasive method can track bone motion accurately but is relatively difficult to implement and may interfere with movement either mechanically or by causing discomfort. Alternatively, non-invasive motion capture methods are more straightforward to implement and could elicit more natural movement by avoiding mechanical interference and discomfort. Non-invasive motion capture methods that have been used for small animals include reflective marker-based infrared motion capture (Gushue et al.

2005), marker-less motion capture from videos (Fiker et al. 2020), and bi-plane fluoroscopy (Koh & Herzog 1998a; Tinga et al. 2018). The two primary tools for measuring ground reaction forces are force plates and pressure mats. Force plates measure the *resultant* forces along 6 degrees of freedom, which requires that only one limb contacts the plate at a time to distinguish forces among limbs (Gushue et al. 2005; Jarrell et al. 2018). Pressure mats, which measure vertical pressure and contact area, are more convenient to use with quadrupedal animals since individual limbs can be distinguished even if multiple limbs contact the mat simultaneously (de Carvalho et al. 2009; Sheldon et al. 2019; Steiner et al. 2019).

Our study was limited in several ways. First, because our pressure mat was relatively narrow (11.2 cm), we could only measure pressure under one hindlimb at a time, which possibly contributed to observed bilateral differences. Additionally, the length of our motion capture setup only allowed us to capture stance phase. In future studies we plan to use a wider pressure mat and longer tunnel with two cameras (one on each side) to capture bilateral gait data over an entire gait cycle. Second, our video-camera-based motion capture setup and custom MATLAB software permitted analysis of 2-D motion in the sagittal plane only. We could more comprehensively characterize hindlimb kinematics with 3-D data obtained either with a multi-camera motion capture system or more advanced software. One such software, DeepLabCut, uses machine learning to track anatomical features without joint markers and can calculate 3-D kinematics from a 2-D video (Mathis et al. 2018a; Mathis et al. 2018b). Third, we tracked marked joint locations on the skin, which are more convenient than bone pins used in the previous rabbit biomechanics study (Gushue et al. 2005) but can move relative to underlying bony landmarks.

Conclusions

In conclusion, we have reported select ground-paw pressure and kinematic data from the intact biological hindlimbs of healthy New Zealand white rabbits. Our results showed that rabbits exhibit a plantigrade gait pattern as claimed in previous literature. vGRF and contact area were highly correlated, resulting in relatively constant pressure during stance. Our results add significantly to the limited existing data on rabbit hindlimb biomechanics. The data reported can be used as an experimental control to quantify the extent to which orthopedic interventions affect rabbit biomechanics. Additionally, knowledge of rabbit hindlimb biomechanics can inform the design and development of orthopedic interventions, such as our prosthesis(Hall et al. 2020b), to improve functional outcomes of patients.

Conflict of Interest Statement

The authors have no conflicts of interest to report.

Acknowledgments

The authors thank Dr. Bryce Burton, Dr. Kelsey Finnie, Dr. Lori Cole, and Chris Carter for veterinary care provided for the rabbits in this study, and the Office of Laboratory Animal Care and Animal Housing Facility staffs at the University of Tennessee, Knoxville for animal care assistance. Thanks to Dr. Katrina Easton for providing constructive feedback on the manuscript. Research reported in this publication was supported by (1) the Eunice Kennedy Shiver National Institute of Child Health & Human Development of the National Institutes of Health under Award Number K12HD073945, (2) NSF CAREER Award #1944001, (3) a seed grant from the University of Tennessee Office of Research and Engagement, and (4) the University of Tennessee Department of Mechanical, Aerospace and Biomedical Engineering start-up funds.

References

Abrams RA, Tsai AM, Watson B, Jamali A, and Lieber RL. 2000. Skeletal muscle recovery after tenotomy and 7-day delayed muscle length restoration. *Muscle Nerve* 23:707-714.

Barbeau H, and Rossignol S. 1987. Recovery of locomotion after chronic spinalization in the adult cat. *Brain research* 412:84-95.

Bensley BA. 1910. *Practical anatomy of the rabbit*: The University Press.

Chang YH, Housley SN, Hart KS, Nardelli P, Nichols RT, Maas H, and Cope TC. 2018. Progressive adaptation of whole-limb kinematics after peripheral nerve injury. *Biol Open* 7. 10.1242/bio.028852

de Carvalho VC, de Alencar Nääs I, Neto MM, and de Souza SRL. 2009. Measurement of pig claw pressure distribution. *biosystems engineering* 103:357-363.

Fiker R, Kim LH, Molina LA, Chomiak T, and Whelan PJ. 2020. Visual Deep Lab Cut: A user-friendly approach to gait analysis. *Journal of Neuroscience Methods*:108775.

Gossman MR, Rose SJ, Sahrmann SA, and Katholi CR. 1986. Length and circumference measurements in one-joint and multijoint muscles in rabbits after immobilization. *Phys Ther* 66:516-520. 10.1093/ptj/66.4.516

Grasso R, Bianchi L, and Lacquaniti F. 1998. Motor patterns for human gait: backward versus forward locomotion. *Journal of neurophysiology* 80:1868-1885.

Gushue DL, Houck J, and Lerner AL. 2005. Rabbit knee joint biomechanics: Motion analysis and modeling of forces during hopping. *Journal of orthopaedic research* 23:735-742. 10.1016/j.orthres.2005.01.005

Hall PT, Bratcher SZ, Stubbs C, Rifkin RE, Grzeskowiak RM, Burton BJ, Greenacre CB, Stephenson SM, Anderson DE, and Crouch DL. 2020a. Fully Implanted Prostheses for Musculoskeletal Limb Reconstruction after Amputation: An In Vivo Feasibility Study. *bioRxiv*:2020.2007.2002.184994. 10.1101/2020.07.02.184994

Hall PT, Bratcher SZ, Stubbs C, Rifkin RE, Grzeskowiak RM, Burton BJ, Greenacre CB, Stephenson SM, Anderson DE, and Crouch DL. 2020b. Fully Implanted Prostheses for Musculoskeletal Limb Reconstruction After Amputation: An In Vivo Feasibility Study. *Annals of biomedical engineering*. 10.1007/s10439-020-02645-3

Jarrell JR, Farrell BJ, Kistenberg RS, Dalton IV JF, Pitkin M, and Prilutsky BI. 2018. Kinetics of individual limbs during level and slope walking with a unilateral transtibial bone-anchored prosthesis in the cat. *Journal of Biomechanics* 76:74-83.

Kadaba MP, Ramakrishnan HK, and Wooten ME. 1990. Measurement of lower extremity kinematics during level walking. *Journal of Orthopaedic Research* 8:383-392.

Koh TJ, and Herzog W. 1998a. Excursion is important in regulating sarcomere number in the growing rabbit tibialis anterior. *The Journal of physiology* 508:267-280.

Koh TJ, and Herzog W. 1998b. Increasing the moment arm of the tibialis anterior induces structural and functional adaptation: implications for tendon transfer. *J Biomech* 31:593-599. 10.1016/s0021-9290(98)00052-9

Li Y, and Hsiao-Wecksler E. 2013. Gait mode recognition and control for a portable-powered ankle-foot orthosis. *IEEE International Conference on Rehabilitation Robotics : [proceedings]* 2013:1-8. 10.1109/ICORR.2013.6650373

Mathis A, Mamidanna P, Abe T, Cury KM, Murthy VN, Mathis MW, and Bethge M. 2018a. Markerless tracking of user-defined features with deep learning. *arXiv preprint arXiv:180403142*.

Mathis A, Mamidanna P, Cury KM, Abe T, Murthy VN, Mathis MW, and Bethge M. 2018b. DeepLabCut: markerless pose estimation of user-defined body parts with deep learning. *Nature neuroscience* 21:1281-1289.

Nagasawa K, Noguchi M, Ikoma K, and Kubo T. 2008. Static and dynamic biomechanical properties of the regenerating rabbit Achilles tendon. *Clin Biomech (Bristol, Avon)* 23:832-838. 10.1016/j.clinbiomech.2008.02.002

Pataky TC. 2010. Generalized n-dimensional biomechanical field analysis using statistical parametric mapping. *Journal of Biomechanics* 43:1976-1982.

Polly PD. 2007. Limbs in mammalian evolution. *Fins into limbs: evolution, development and transformation*:245-268.

Ponten E, and Friden J. 2008. Immobilization of the rabbit tibialis anterior muscle in a lengthened position causes addition of sarcomeres in series and extra-cellular matrix proliferation. *J Biomech* 41:1801-1804. 10.1016/j.jbiomech.2008.03.006

Reddy GK, Stehno-Bittel L, and Enwemeka CS. 1998. Laser photostimulation of collagen production in healing rabbit Achilles tendons. *Lasers Surg Med* 22:281-287. 10.1002/(sici)1096-9101(1998)22:5<281::aid-lsm4>3.0.co;2-l

Reddy NP, and Gupta V. 2007. Toward direct biocontrol using surface EMG signals: control of finger and wrist joint models. *Medical Engineering & Physics* 29:398-403. 10.1016/j.medengphy.2005.10.016

Sheldon JD, Adkesson MJ, Allender MC, Bailey RS, Langan JN, and Chinnadurai SK. 2019. Evaluation of a pressure sensitive walkway for objective gait analysis in normal and arthritic domestic ducks (Cairina moschata domestica). *PloS one* 14:e0220468.

Sjostrom M, Wahlby L, and Fugl-Meyer A. 1979. Achilles tendon injury. 3. Structure of rabbit soleus muscles after immobilization at different positions. *Acta Chir Scand* 145:509-521.

Steiner R, Dhar M, Stephenson SM, Newby S, Bow A, Pedersen A, and Anderson DE. 2019. Biometric Data Comparison Between Lewis and Sprague Dawley Rats. *Frontiers in Veterinary Science* 6. 10.3389/fvets.2019.00469

T K. 1996. Correlation between the morphology of the feet and muscle fiber composition in the anterior tibial muscle. *Anthropological Science* 104:1-14.

Tinga S, Kim SE, Banks SA, Jones SC, Park BH, Pozzi A, and Lewis DD. 2018. Femorotibial kinematics in dogs with cranial cruciate ligament insufficiency: a three-dimensional in-vivo fluoroscopic analysis during walking. *BMC veterinary research* 14:1-9.

Wannop J, Worobets JT, and Stefanyshyn D. 2012. Normalization of ground reaction forces, joint moments, and free moments in human locomotion. *Journal of Applied Biomechanics* 28 6:665-676.

Winiarski S, and Rutkowska-Kucharska A. 2009. Estimated ground reaction force in normal and pathological gait. *Acta of Bioengineering & Biomechanics* 11.

List of Illustrations

Figure 1. Testing setup used to collect motion capture data. (1) Tekscan Very HR Walkway 4 to collect pressure data. **(2)** Acrylic tunnel used to guide and constrain rabbit movement. **(3)** 60 Hz Camera recorded sagittal plane kinematics. **(4)** Black ink markers on the sagittal plane joints based on bony landmarks.

Figure 2. Motion capture analysis of the sagittal plane videos allows for measurement of the rabbit hindlimb kinematics. Frame-by-frame top hat morphology allows for detection of joint markers. Joint segments (orange) can be drawn between the centroids of the joint segments. From these joint angles we calculate the ankle angle (yellow) and the angle between the foot and ground (blue) through the dot product of unit vectors of the joint and ground segments. The ground (dashed blue) is determined as the horizontal line segment that intersects the MTP joint.

Figure 3. Example of strike box isolation of the contact foot using the Tekscan Walkway. Through the Tekscan software we can isolate the force and contact area of a specific hindlimb foot strike.

Figure 4. Ground reaction data throughout stance phase. (Left) Vertical ground reaction force of the rabbit hindlimb throughout stance. vGRF has a bimodal pattern at 25% and 75% of stance phase. **(Middle)** Contact area of the rabbit hindlimb throughout stance. Similar to vGRF data, the contact area has a bimodal pattern at 25% and 75% of stance phase. vGRF and contact area have a Pearson's correlation coefficient of 0.986. **(Right)** Contact pressure of the

rabbit hindlimb throughout stance phase. Rabbits maintain a fairly constant pressure throughout the entirety of stance?

Figure 5. Contact Area of the rabbit hindlimb throughout stance phase. The left graph shows the comparison of the contact area between the right and left hindlimb throughout stance phase. The numbered timepoints correspond to contact area screenshots from a representative trial of rabbit stance.

Figure 6. Joint Kinematics of the rabbit hindlimb throughout stance phase. Foot and ankle angles throughout stance phase. Rabbit stance can be broken down into two phases, loading response and propulsion, based on the timepoint of the minimum ankle angle.

Figure 7. Normalized joint tracking and kinematic comparison between knee trajectories. (Left) Recreation of rabbit stance using normalized limb segments. Each hindlimb location represents hindlimb kinematics at each 10% of stance. Representations of hindlimb anatomy juxtaposed at foot strike and toe off for reference. **(Right)** Using the normalized hindlimb kinematics we can recreate the kinematics and trajectories of both the ankle and knee joint throughout stance.

Figure 8. Euclidian distance between right and left normalized joint positions throughout stance. (Left) Comparing the knee joint trajectories throughout stance allows for visual comparison between hindlimbs. There is minimal noticeable difference between the right and left knee trajectories measured in this study. **(Right)** Euclidean distance between the right and

left normalized knee position throughout stance. The knee position showed statistically significant difference throughout the entirety of stance.

Figure 1

Testing setup used to collect motion capture data.

Figure 1. Testing setup used to collect motion capture data. (1) Tekscan Very HR Walkway 4 to collect pressure data. (2) Acrylic tunnel used to guide and constrain rabbit movement. (3) 60 Hz Camera recording sagittal plane kinematics. (4) Black ink marking the sagittal plane joints based on bony landmarks.

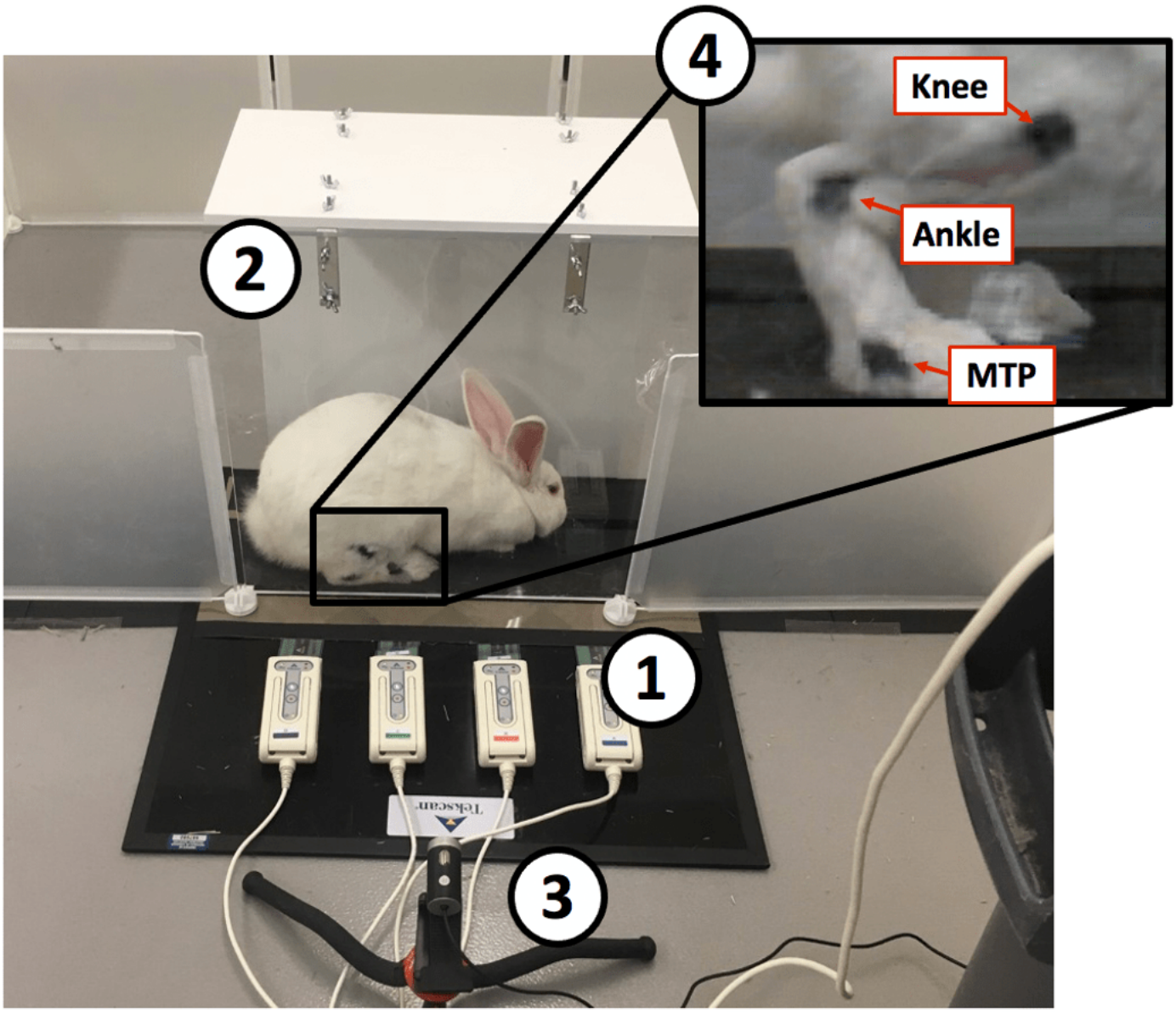

Figure 2

Motion capture analysis of the sagittal plane videos allows for measurement of the rabbit hindlimb kinematics.

Frame-by-frame top hat morphology allows for detection of joint markers. Joint segments (orange) can be drawn between the centroids of the joint segments. From these joint angles we calculate the ankle angle (yellow) and the angle between the foot and ground (blue) through the dot product of unit vectors of the joint and ground segments. The ground (dashed blue) is determined as the horizontal line segment that intersects the MTP joint.

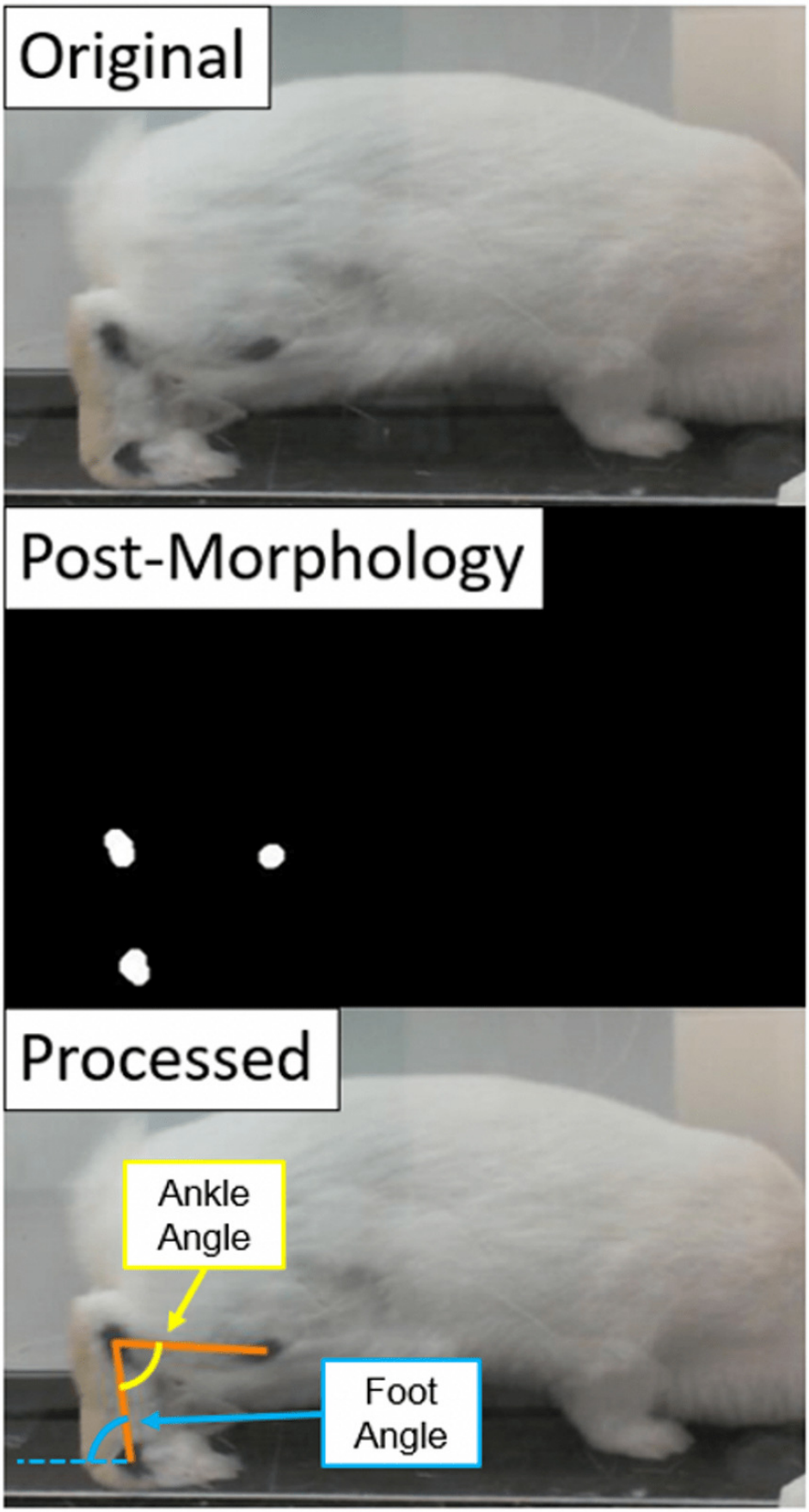
Original
Post-Morphology
Processed
Ankle Angle
Foot Angle

Figure 3

Example of strike box isolation of the contact foot using the Tekscan Walkway.

Figure 3. Example of strike box isolation of the contact foot using the Tekscan Walkway. Through the Tekscan software we can isolate the force and contact area of a specific hindlimb foot strike.

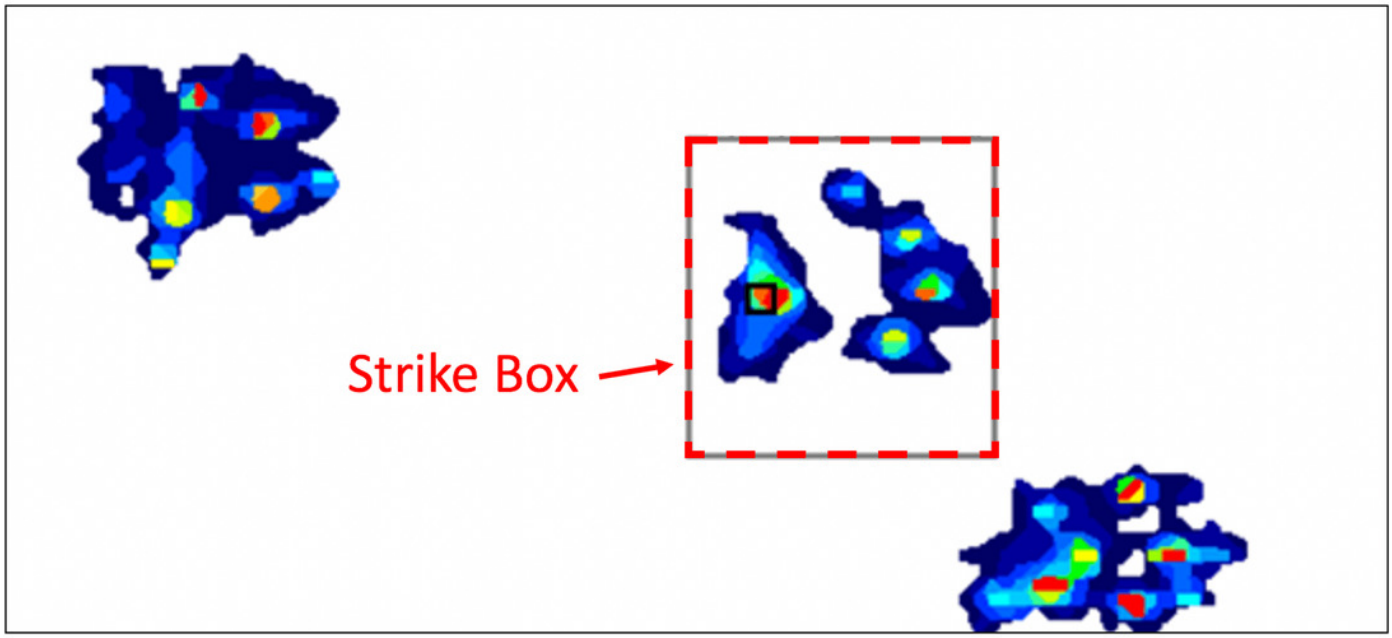

Figure 4

Ground reaction data throughout stance phase.

Figure 4. Ground reaction data throughout stance phase. (Left) Vertical ground reaction force of the rabbit hindlimb throughout stance. vGRF has a bimodal pattern at 25% and 75% of stance phase. (Middle) Contact area of the rabbit hindlimb throughout stance. Similar to vGRF data, the contact area has a bimodal pattern at 25% and 75% of phase. vGRF and contact area have a Pearson's correlation coefficient of 0.986. (Right) Contact pressure of the rabbit hindlimb throughout stance phase. Rabbits maintain a fairly constant pressure throughout the entirety of stance?

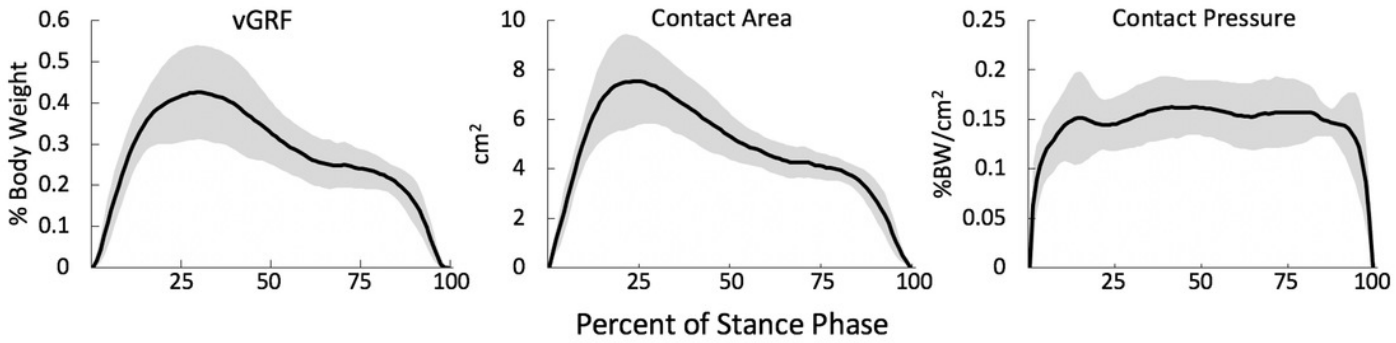

Figure 5

Contact Area of the rabbit hindlimb throughout stance phase.

The left graph shows the comparison of the contact area between the right and left hindlimb throughout stance phase. The numbered timepoints correspond to contact area screenshots from a representative trial of rabbit stance.

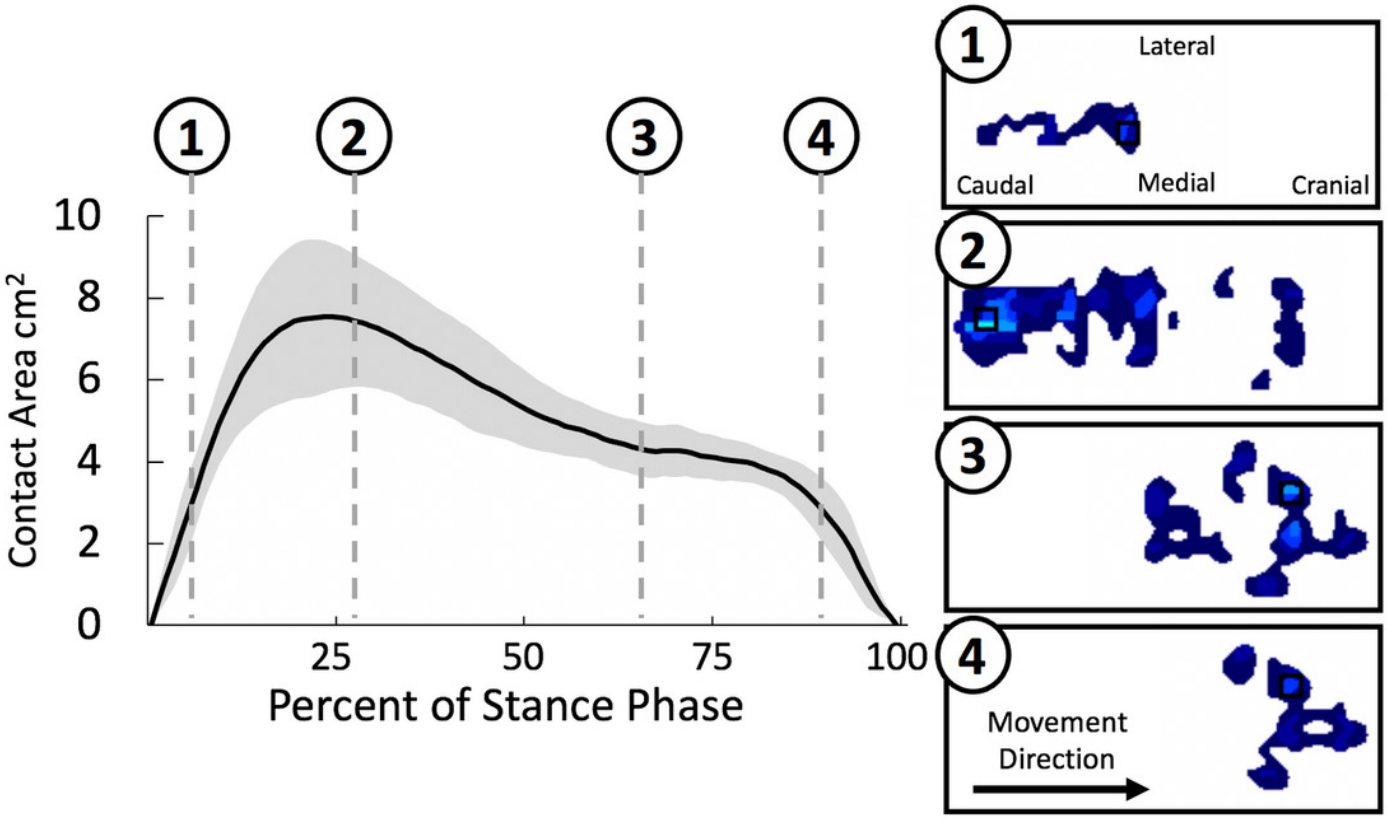

Figure 6

Joint Kinematics of the rabbit hindlimb throughout stance phase.

Foot and ankle angles throughout stance phase. Rabbit stance can be broken down into two phases, loading response and propulsion, based on the timepoint of the minimum ankle angle.

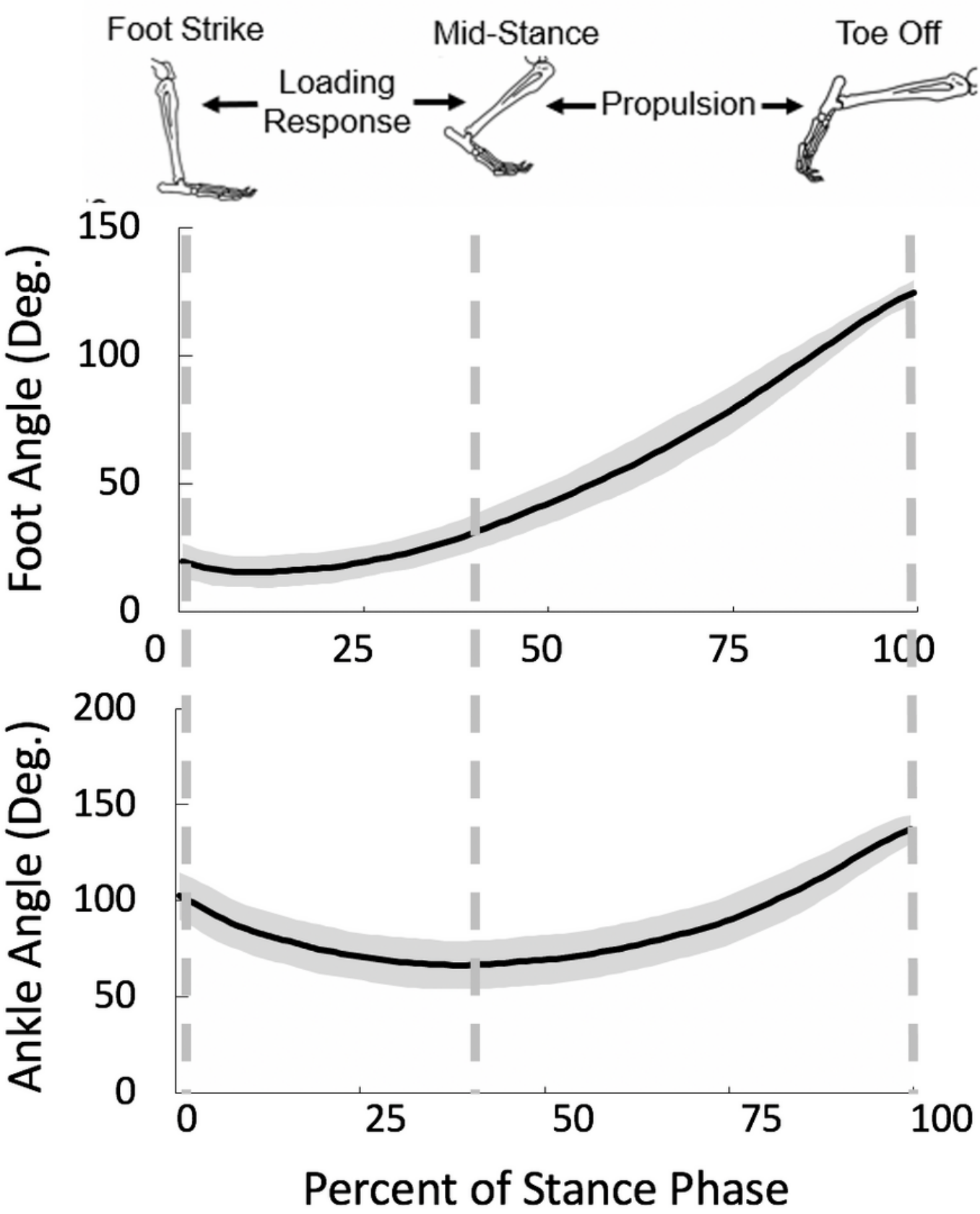
Foot Strike
Mid-Stance
Toe Off
Loading Response
Propulsion
Foot Angle (Deg.)
150
100
50
0
0
25
50
75
100
Ankle Angle (Deg.)
200
150
100
50
0
0
25
50
75
100
Percent of Stance Phase

Figure 7

Normalized joint tracking and kinematic comparison between knee trajectories.

Figure 7. Normalized joint tracking and kinematic comparison between knee trajectories. (Left) Recreation of rabbit stance using normalized limb segments. Each hindlimb location represents hindlimb kinematics at each 10% of stance. Representations of hindlimb anatomy juxtaposed at foot strike and toe off for reference. (Right) Using the normalized hindlimb kinematics we can recreate the kinematics and trajectories of both the ankle and knee joint throughout stance.

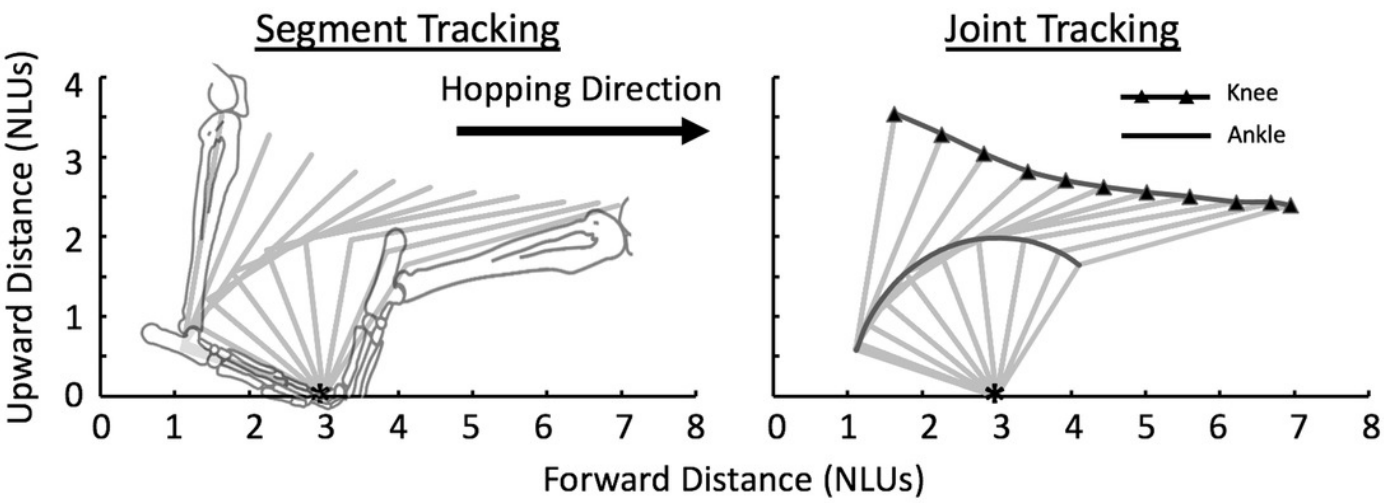

Figure 8

Euclidian distance between right and left normalized joint positions throughout stance.
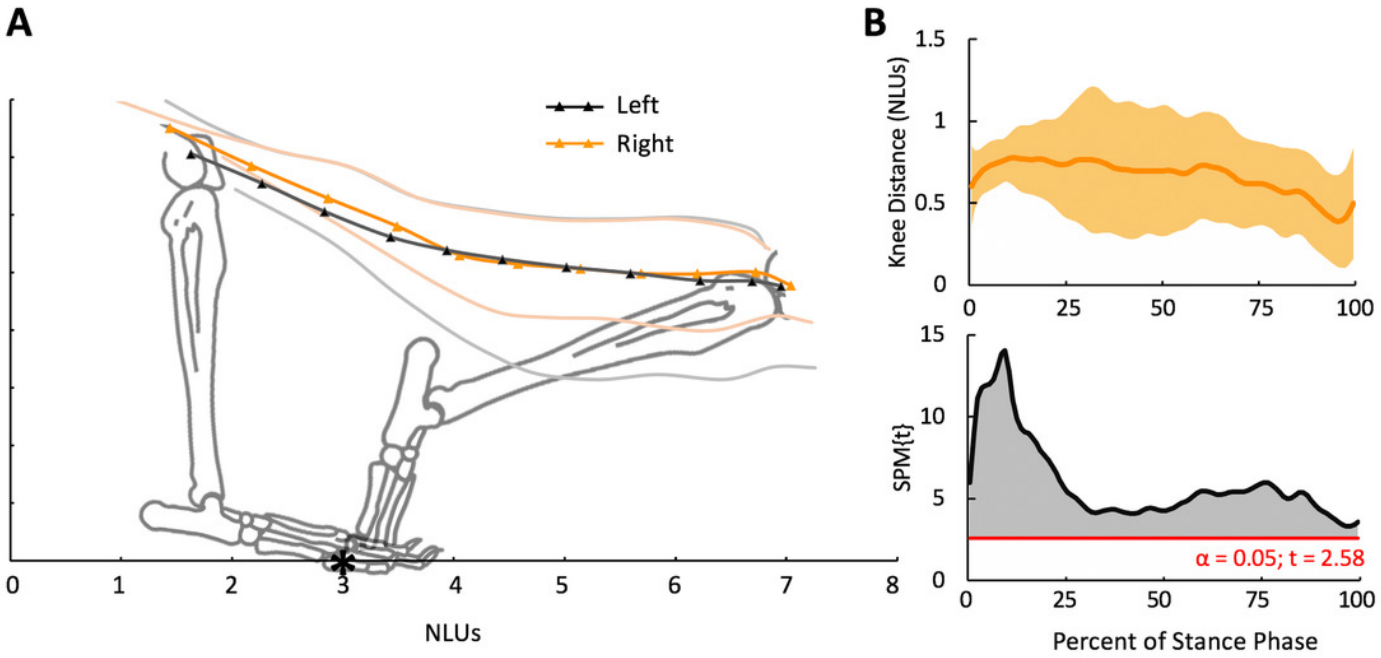
Figure 8. Euclidian distance between right and left normalized joint positions throughout stance. (Left) Comparing the knee joint trajectories throughout stance allows for visual comparison between hindlimbs. There is minimal noticeable difference between the right and left knee trajectories measured in this study. (Right) Euclidean distance between the right and left normalized knee position throughout stance. The knee position showed statistically significant difference throughout the entirety of stance.